Environmental Science & Technology

Article

pubs.acs.org/est

Biogeochemical Processes Governing Natural Pyrite Oxidation and Release of Acid Metalliferous Drainage

Ya-ting Chen,[†,‡,§] Jin-tian Li,[†,§] Lin-xing Chen,[†] Zheng-shuang Hua,[†] Li-nan Huang,[†] Jun Liu,[†] Bi-bo Xu,[†] Bin Liao,[†] and Wen-sheng Shu*[,†]

[†]State Key Laboratory of Biocontrol and Key Laboratory of Biodiversity Dynamics and Conservation of Guangdong Higher Education Institutes, School of Life Sciences, Sun Yat-sen University, Guangzhou 510275, PR China

[‡]Guangdong Key Laboratory of Agricultural Environment Pollution Integrated Control, Guangdong Institute of Eco-Environmental and Soil Sciences, Guangzhou 510650, PR China

Supporting Information

ABSTRACT: The oxidative dissolution of sulfide minerals (principally pyrite) is responsible for the majority of acid metalliferous drainage from mine sites, which represents a significant environmental problem worldwide. Understanding the complex biogeochemical processes governing natural pyrite oxidation is critical not only for solving this problem but also for understanding the industrial bioleaching of sulfide minerals. To this end, we conducted a simulated experiment of natural pyrite oxidative dissolution. Pyrosequencing analysis of the microbial community revealed a distinct succession across three stages. At the early stage, a newly proposed genus, *Tumebacillus* (which can use sodium thiosulfate and sulfite as the sole electron donors), dominated the microbial community. At the midstage, *Alicyclobacillus* (the fifth most abundant genus at the early stage) became the most dominant genus, whereas *Tumebacillus* was still ranked as the second most abundant. At the final stage, the microbial community was dominated by *Ferroplasma* (the tenth most abundant genus at the early stage). Our geochemical and mineralogical analyses indicated that exchangeable heavy metals increased as the oxidation progressed and that some secondary sulfate minerals (including jarosite and magnesiocopiapite) were formed at the final stage of the oxidation sequence. Additionally, we propose a comprehensive model of biogeochemical processes governing the oxidation of sulfide minerals.

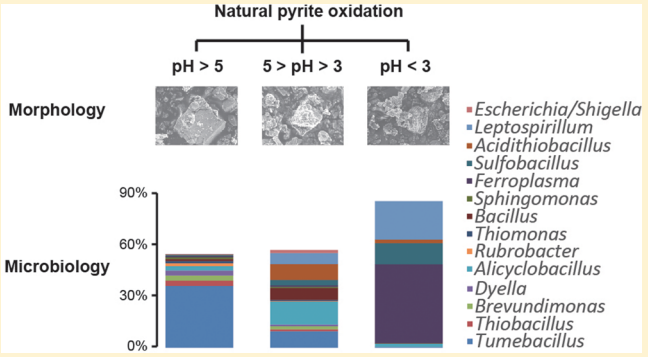

INTRODUCTION

The oxidation of sulfide minerals (principally pyrite) plays a key role in the biogeochemical cycling of iron and sulfur.[1] However, this oxidation process may have harmful consequences for the environment, because it can produce excessive quantities of acidic, metal-rich drainage from mine sites.[2] In the past two decades, many efforts have been made to improve our understanding of the biogeochemical processes involved in oxidation of sulfides,[3−6] which is essential not only for developing efficient approaches for dealing with the environmental pollution caused by oxidation but also for bioleaching of sulfide minerals. As the most abundant sulfide mineral in nature, the oxidation of pyrite (FeS_2) has been investigated more extensively than any other sulfide mineral.[7,8] Based on geochemical and mineralogical data from many previous studies, the mechanism of chemical oxidation of FeS_2 has been proposed, summarized by the following equations:[9]

$$FeS_2 + 6Fe^{3+} + 3H_2O \rightarrow S_2O_3^{2-} + 7Fe^{2+} + 6H^+ \quad (1)$$

$$S_2O_3^{2-} + 8Fe^{3+} + 5H_2O \rightarrow 2SO_4^{2-} + 8Fe^{2+} + 10H^+ \quad (2)$$

In this thiosulfate mechanism, the Fe−S_2 bond can only be broken by the attack of Fe^{3+}. Thus, Fe^{3+} has been considered as the most important oxidant for FeS_2 dissolution in nature.[9]

Geomicrobiological studies on the oxidation of mine tailings and acid mine drainage (AMD) have shown that some Fe-oxidizing microorganisms, such as *Acidithiobacillus ferrooxidans*, *Leptospirillum ferrooxidans*, and *Ferroplasma acidiphilum*, can greatly enhance the oxidation of pyrite, by oxidizing Fe^{2+} and rapidly replenishing the oxidant Fe^{3+}.[8] In addition, some S-oxidizing microorganisms, such as *Acidithiobacillus thiooxidans* and *Acidithiobacillus caldus*, have been also found to be strongly involved in pyrite oxidation, wherein they can generate sulfuric acid via oxidation of intermediary sulfur compounds.[8]

Despite these important advances, we still have a relatively limited understanding of the elaborate mechanisms responsible for the oxidation of the naturally occurring mineral pyrite in the environment. In particular, very little is known about the

Received: January 14, 2014
Revised: April 14, 2014
Accepted: April 14, 2014
Published: April 14, 2014

ACS Publications © 2014 American Chemical Society

potential shifts in community structure of microbes associated with the oxidation. There are several underlying reasons for this. First, the oxidation of natural pyrite in the environment involves a set of complex biogeochemical processes in which many microbes may have different roles.[10] However, a majority of previous studies have attempted to address these processes using either pure pyrite or pure cultures of individual microbes.[11,12] In some cases, where natural pyrite and mixed cultures of several microbes were used, pyrite was added in reactors at very low concentrations (<10%).[13,14] It is apparent that the experimental conditions of these previous studies did not reflect the real situations of natural pyrite oxidation in the field. Second, characterizing the biogeochemical processes involved in oxidation of natural pyrite will require the assay of a series of samples that may represent different stages of the oxidation process through a combination of geochemical, mineralogical, and microbiological approaches. The typical method for profiling a microbial community based on 16S rDNA clone library analysis is laborious, costly, and time-consuming, which diminishes its utility in studies that may require a relatively large sample size.[15] Thus, there have been very few good empirical studies that couple the geochemical and/or mineralogical measurements of pyrite oxidation with the shifts in community composition of the microbes associated.[7,10] Third, mine sites are highly disturbed ecosystems, and the oxidation process of natural pyrite in these ecosystems can be frequently interrupted by various random factors. This implies that it is a challenge to track the oxidation process in the field and to obtain appropriate samples representing different stages of the process. Lastly, most previous studies addressing the biogeochemical processes involved in natural pyrite oxidation by analyzing environmental samples have focused on either pyrite-containing mine tailings or AMD rather than pyrite per se.[3−6,16,17]

It is only quite recently that next-generation high-throughput pyrosequencing has been applied to analyze the microbial community composition of environmental samples.[18] This new technology eliminates the need for laborious cloning of DNA, making possible the sequencing of DNA from many different samples simultaneously, so allowing researchers to characterize many microbial communities more rapidly and more cheaply than previously possible.[19]

In the present study, we used pyrosequencing to characterize microbial communities associated with the oxidation of natural pyrite and thereby further address the linkages between the geochemistry, mineralogy, and microbiology of the oxidation process. Specifically, the objectives of this study were to (1) investigate the potential shifts in microbial community composition of samples representing different stages of natural pyrite oxidation; (2) determine the differences between the samples in geochemical and mineralogical characteristics; and (3) explore the biogeochemical processes governing natural pyrite oxidation. For these purposes, we conducted a simulation experiment of pyrite oxidation in the field using naturally occurring mineral pyrite but without the intentional addition of microbes under greenhouse conditions, which was expected to reduce disturbances to the oxidation process.

MATERIALS AND METHODS

Simulation Experiment. Owing to the difficulty of tracking natural pyrite oxidation in the field, we conducted a simulation experiment with natural pyrite under greenhouse conditions. The experiment was performed with an artificial system established on June 26, 2009 in a ventilated greenhouse on the Sun Yat-sen University campus. A 1 × 1 × 1 m cement-lined pit was constructed and then filled with approximately 5 t of natural pyrite particles (<5 cm in diameter) collected from Yunfu Pyrite Mine, which is the richest pyrite mine in China.[20] Specifically, pyrite content for the natural pyrite used in this study was 23%. Four PVC pipes (approximately 15 cm in diameter and 1.2 m in height) were inserted into four holes located in the four corners of the pit (Supporting Information, Figure S1). To simulate the oxidation of natural pyrite in the environment, we exposed the pyrite to wetting and drying cycles, with the pyrite partly immersed in the fluid during the wetting process. At the beginning of each cycle, sterilized water was added to the pit through the pipes (with each pipe received near equal amount of water per time, Figure S1). Unlike previous studies, intentional addition of microbes was excluded from this experiment, because we believed that such a design better reflects the real field situation.

Sampling. We attempted to track the temporal dynamics of oxidation of the natural pyrite and collect representative samples at different stages of the oxidation process. Thus, we determined the pH of the pyrite weekly, given that a direct consequence of pyrite oxidation is a decrease in pH.[21] However, we did not observe any remarkable decrease 2 years after the experiment was set up, which further confirmed the difficulty of tracking the oxidation process of natural pyrite. To reduce the cost of time and labor, we measured the pH of the pyrite each month from July 2011. The expected gradual decrease in pH was not recorded; instead, a sudden decrease in pH (<3) was recorded at the end of a drying process in November 2011 (Figure S1). At the same time, the characteristic yellowish-red deposits ("yellow boy"), which are expected to be formed when the pyrite oxidation begins, were observed in some surfaces of the pyrite (Figure S1).[22,23] In such circumstances, we had to employ a space-for-time substitution sampling approach. Specifically, to obtain samples that were likely to represent different stages of the pyrite oxidation process, a total of 29 samples showing no, slight, and strong signs of oxidation (principally color, texture, and degree of concretion)[24] was collected in November 21, 2011. Samples were collected from the top 1 cm surface with sterile spoons, transferred to sterile culture bottles, stored in ice boxes, transported to the laboratory, and stored at 4 °C for subsequent analyses. We divided our samples into three groups according to their pH (see Table 1 for more details). These groups of samples were used to represent the following three stages of the pyrite oxidation process: the early stage (pH > 5), 8 samples; the mid stage (3 < pH < 5), 6 samples; the final stage (pH < 3), 15 samples. This was done largely based on a notion that the mine tailings with pH < 3 and pH > 5 can be considered as "actively oxidizing" and "unoxidized", respectively.[25] It should be noted that the three groups of our samples showed a random spatial distribution within our study area (i.e., the sampling zone within the pit, Figure S1). In this sense, our study seemed to be different from those typical studies using the "space-for-time" approach,[26−28] because samples of the latter often show an apparent spatial distribution (i.e., nonrandom) pattern within the study areas. This discrepancy, however, did not undermine the assumption of the "space-for-time" approach, because we demonstrated that our samples did show substantial differences in chemical and mineralogical characteristics (see the Results and Discussion section for more details). These differences were comparable to those observed

for temporal sequences in previous studies involving the oxidation of pyrite-containing materials.[7,29−32] There were at least two possible reasons for the random spatial (i.e., heterogeneous) distribution of our samples. On the one hand, there is evidence that attachment of Fe-oxidizing microbe cells to a mineral surface can increases the rate of oxidation of sulfide minerals,[8] although such an attachment is a random process (as exemplified by the random distribution of the cell-sized and -shaped dissolution pits in the mineral surface).[32] On the other hand, burrowing into the pre-existing cracks, fissures, and pores in sulfide minerals can facilitate the attachment of Fe-oxidizing microbes to the mineral surface; however, this burrowing process also seems to be random due to the fact that other microbes can also occupy the "niche" space.[33−35]

Chemistry. Electrical conductivity (EC) and pH were measured in situ by use of specific electrodes. Redox potential (Eh) was determined using an Ag/AgCl reference electrode. Ferrous and ferric ions were measured immediately after sampling by an UV colorimetric assay with 1,10-phenanthroline at 530 nm wavelength. Moisture content was measured as the difference in sample weight before and after drying at 105 °C for 12 h. The samples were air-dried for analysis of other geochemical characteristics. Sulfate was extracted by deionized water and detected using a 1 mM $NaHCO_3$/8 mM Na_2CO_3 eluent at a 1.0 mL min^{-1} flow rate through an IonPac AS14A column. Total sulfur was oxidized to sulfate by $Mg(NO_3)_2$ and determined by a $BaSO_4$-based turbidimetric method. Total C was determined using an elemental analyzer (Vario EL, Elementar, Hanau, Germany). Total N was measured by Kjeldahl digestion procedures, and total P was determined colorimetrically by the ascorbic acid method at 700 nm wavelength. Total concentrations of heavy metals (Fe, Pb, Zn, Cu, Cd, and Mn) were determined by inductively coupled plasma optical emission spectrometry (ICP-OES; Optima 2100DV, PerkinElmer, Massachusetts, U.S.A.) after digestion with an HNO_3/HCl/HF mixture. Five fractions of heavy metals (exchangeable, bound to carbonates, bound to Fe−Mn oxides, bound to organic matter, and residual) were extracted[36] and measured by ICP-OES.

X-ray Diffraction (XRD). For each sample, 1 g of air-dried subsample was ground and homogenized for XRD analysis. X-ray diffractions were performed with a Rigaku Model D/Max-IIIA Powder diffractometer (Cu Kα radiation, operated at 35 kV and 25 mA) in order to identify the crystalline phase in the samples. Continuous scans were taken over a 2θ range of 5° to 80° at a speed of 3° min^{-1}. The analysis of diffraction data was carried out using JADE 5.0 software (Materials Data, Inc., Livermore, U.S.A.) and the PDF4+ database (ICSD). We used a standard (i.e., the reference intensity ratio, RIR) method for quantitative analysis of every phase in our samples as shown by XRD. The RIR is defined as the ratio of the intensity of the strongest peak of a phase to that of an internal standard (i.e., corundum) when the phase is mixed 1:1 by weight with corundum.[37,38]

Scanning Electron Microscopy (SEM). To reveal potential changes in surface morphology of pyrite samples representing different oxidation stages, a fraction of each sample was air-dried, homogenized, carbon-coated, and observed using a field-emission scanning electron microscopy (model JSM-6330F, JEOL, Tokyo, Japan).

DNA Extraction and Bar-Coded Pyrosequencing. An indirect method was employed to recover microbial cells from the samples.[39] Then the community DNA of microbes was extracted using a FastDNA Spin kit (Bio 101, Carlsbad, CA, U.S.A.) according to the manufacturer's protocol. We used the F515 and R806 primer set that was designed to amplify the bacterial and archaeal 16S rRNA genes V4 hypervariable region.[40] The R806 primer contained an 8-bp bar-code sequence. PCR amplification (30 μL) was conducted in triplicate under the following conditions: 30 cycles of denaturation at 94 °C for 30 s, annealing at 50 °C for 1 min, and extension at 72 °C for 1 min, with a final extension at 72 °C for 10 min. The PCR products from individual samples were combined in equimolar ratio in a single tube,[41] purified by a QIAquick Gel Extraction Kit (Qiagen, Chatsworth, CA, U.S.A.), and the composite DNA was sequenced using the GS FLX Titanium pyrosequencing platform (454 Life Sciences Corp., CT, U.S.A.).

Processing of 454 Pyrosequencing Data. Data were processed and analyzed following the pipelines of Mothur[42] and Quantitative Insights Into Microbial Ecology (QIIME).[43] The chimeric and low quality sequences were identified and removed, whereas the 8 bp bar code was examined in order to assign sequences to individual samples. The phylotypes were defined at the sequence similarity level of 97%, and a representative sequence from each phylotype was aligned using NAST.[44] Taxonomic classification of each phylotype was determined using the Ribosomal Database Project (RDP) with a minimum confidence of 80%.[45] The number of quality sequences for individual samples ranged from 634 to 3883. To reduce the potential bias of variation in sequencing depth, 634 randomly selected sequences were used for each sample for further analyses (OTU richness, phylogenetic diversity, Chao1, Shannon and Simpson index). Sequences were compared using BLAST against NCBI-nr database with default parameters and have been deposited in the European Nucleotide Archive under accession number ERR445557. The sequence similarities between the dominant genera (whose average relative abundances >1% in at least one stage) in this study and the reference species (sequences) were provided in Table S1.

Statistical Analysis. All statistical analyses were performed using SPSS 18.0 software (SPSS, Inc., Chicago, U.S.A.). One-way ANOVA was carried out for the three pyrite oxidation stages to test for differences in geochemical, mineralogical, and microbial characteristics. Differences between means were tested by least significant difference (LSD) at the 5% level. To explore any correlations between the geochemical and the microbial characteristics of our samples, a robust multivariate analysis method (canonical correspondence analysis, CCA)[46] was used (see the Supplementary Note in Supporting Information for more details). This method was chosen, because relationships between species abundance or occurrence probability and environmental variables are often unimodal, which makes other linear-based multivariate methods unsuitable.[46]

RESULTS AND DISCUSSION

Geochemical Characteristics of Samples Representing the Three Stages of Pyrite Oxidation. The total S contents of the pyrite samples were higher than 20% (Table 1), showing that the natural pyrite used in this study can be considered as midgrade pyrite. The pyrite was further characterized with low contents of C, N, and P (Table 1), indicating nutrient deficiencies. At the early stage of oxidation, pyrite showed an average pH value of 5.6, which dropped dramatically to 2.5 at the final stage (pH < 3, Table 1). In contrast, EC, Eh,

Table 1. Geochemical Properties (means ± SEs) of Samples Representing the Three Stages of the Pyrite Oxidation[a]

sample	pH	EC	Eh	moisture content	T-S	T-Fe	T-C	SO_4^{2-}	Fe^{3+}	Fe^{2+}	T-N	T-P
pH > 5	5.6 ± 0.19a	1981 ± 109c	135 ± 46b	2.4 ± 1.1b	25 ± 1a	34 ± 1a	1.2 ± 0.1a	25 ± 6b	2.5 ± 0.4b	2.3 ± 0.9b	182 ± 30ab	17 ± 7a
5 > pH > 3	4.2 ± 0.22b	4065 ± 230b	178 ± 69b	2.3 ± 0.3b	22 ± 1a	32 ± 1a	1.2 ± 0.1a	27 ± 7b	4.6 ± 0.4b	4.3 ± 1.1a	219 ± 51a	13 ± 4a
pH < 3	2.5 ± 0.24c	5927 ± 64a	667 ± 69a	12 ± 1a	24 ± 1a	31 ± 1a	1.0 ± 0.1a	69 ± 6a	14 ± 1a	2.0 ± 0.2b	105 ± 13b	13 ± 2a

[a]Within each column, mean values followed by different lower-case letters after SEs are significantly different from each other ($p < 0.05$, LSD). EC, electrical conductivity ($\mu S\ cm^{-1}$); Eh, redox potential (mV); moisture content (%); T-S, total sulphur (%); T-Fe, total Fe (%); T-C, total carbon (%); SO_4^{2-} ($g\ kg^{-1}$); Fe^{3+} and Fe^{2+} ($g\ kg^{-1}$); T-N, total nitrogen ($mg\ kg^{-1}$); T-P, total phosphorus ($mg\ kg^{-1}$).

concentrations of SO_4^{2-} and Fe^{3+}, and moisture content increased significantly as oxidation progressed, being consistent with the results of the previous studies addressing pyrite oxidation using pure pyrite, pure cultures of microbes, or pyrite-containing mine tailings.[10,16,17,29−32,47−50] Fe^{2+} concentrations did not show any significant trend (Table 1), which was likely due to the fact that Fe^{2+} was easily oxidized. In addition, the molar ratio of net Fe^{2+} to SO_4^{2-} decreased from 0.158 at the early stage to 0.05 at the final stage, which was much lower than the theoretical expected value (i.e., 0.5) at steady state, and indicated a stronger extent of secondary sulfate mineral formations and reoxidization Fe^{2+} at the final stage.

It has frequently been reported that pyrite oxidation is associated with increased mobility of the heavy metals existing in the crystalline structures of the mineral.[16,17,49,51−53] In agreement with this, our results showed that the percentages of exchangeable fractions of Pb, Zn, Cd, and Mn increased significantly ($p < 0.05$) as the oxidation progressed (Figure S2). On the other hand, no clear trend was found for the percentages of these heavy metals in the residual fraction, indicating that this fraction was not easily oxidized.[36]

Mineralogical Characteristics of Samples Representing the Three Stages of Pyrite Oxidation. The XRD analysis indicated that the surface of the pyrite samples at the early and mid stages of oxidation consisted largely of calcite, quartz, pyrite, and gypsum (Table S2), which was similar to the results from an investigation of the mineralogical composition of samples collected from Río Tinto deposits in Spain.[54] It should be noted that the relative content of pyrite (21%) recorded here was relatively low, considering that the total S content of the pyrite samples was >20% (Table 1). A possible reason for this was that the majority of pyrite in the surface of the mineral was oxidized.[50] At the final stage, the relative content of pyrite was not significantly ($p > 0.05$) different from those of the early and mid stages. However, the relative content of calcite decreased markedly from 23% at the early stage to 14% at the final stage (Table S2), in agreement with the finding that chemical oxidation of pyrite was able to increase the dissolution of calcite.[55] In contrast, the relative content of gypsum was found to increase dramatically from 8% at the early stage to 27% at the final stage (Table S2). This result was expected, because it has been proposed that the Ca^{2+} and SO_4^{2-} within the gypsum from the sulfide-rich environments are derived from pH-buffering reactions between pore water and Ca-bearing carbonates and the oxidation of sulfide minerals, respectively.[52] Indeed, gypsum has been considered as a common initial cementing phase within the cemented layers in sulfide-bearing environments,[52,56] where pyrite oxidation occurs naturally. It has been also noted, however, that the dominance of gypsum is likely to be replaced with that of jarosite, because the pH decrease associated with pyrite oxidation favors the precipitation of jarosite.[24,52] In agreement with this, jarosite (with a relative content of 10%) was detected at the final stage but not at early and mid stages (Table S2). Although goethite was not detected in this study, it should be noted that the precipitation of secondary minerals (such as gypsum, jarosite, and goethite) can lead to an incomplete oxidation of the pyrite, because the formation of either a gypsum/jarosite-based cement or a goethite-rich cement is able to restrict the diffusion of the oxidizing agent through the pyrite.[24,52] Additionally, another secondary sulfate mineral (magnesiocopiapite), which has been reported as a component of precipitation in environments where pyrite oxidation has

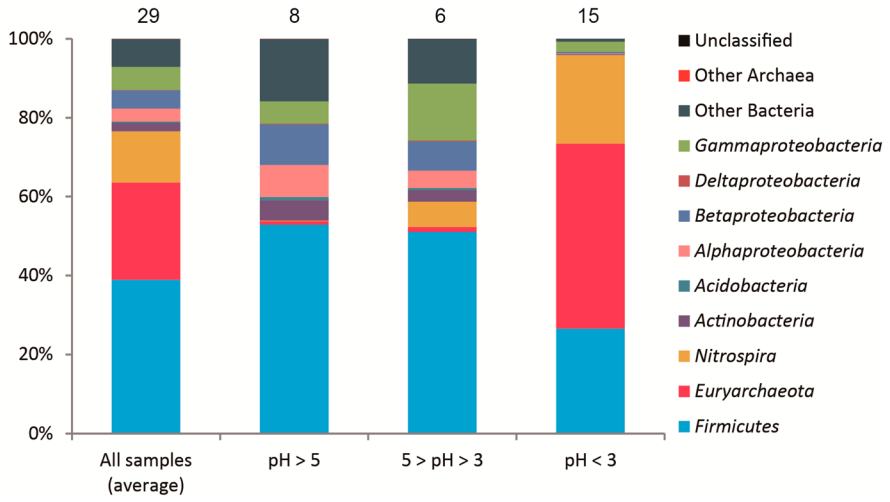

Figure 1. Relative abundance (%) of the dominant microbial phyla in all the samples and those representing the three stages of pyrite oxidation. Those phyla with an average relative abundance of >1% in at least one stage were defined as dominant ones. The figures above the bars indicate the sample size.

occurred,[54,57,58] was recorded at the final stage with a relative content of 8%, although it was not detected at the earlier stages (Table S2). Further studies are clearly needed to elucidate the effects of various secondary minerals on the oxidation of natural pyrite.

Representative SEM photomicrographs of the pyrite samples are shown in Figure S3. The cubic pyrite crystal was relatively complete and the particle surface was smooth at the early stage, but the surface became increasingly rough as the oxidation progressed, which is consistent with SEM observations of the mineralogy of pyrite oxidation by different chemical oxidants made by others.[32,59] This change in surface morphology, in turn, would have important effects on natural pyrite oxidation, because oxidative dissolution of pyrite-rich mine tailings was reported to be sensitive to surface imperfections and changes in surface area.[10] The small brighter patches in the surfaces of pyrite at mid and final stages were likely attributed to the secondary sulfate minerals (Figure S3) precipitated onto the cubic pyrites crystal after evaporation.[7,60] Additionally, some surfaces of pyrite at the final stage contained deep euhedral pits, which are considered as typical etched-pitted texture of pyrite results from active oxidation. A similar observation using SEM has been reported for the mineralogical characteristics of the oxidized pyrite AMD sediments at Iron Mountain (California, U.S.A.).[60]

Microbiological Characteristics of Samples Representing the Three Stages of Pyrite Oxidation. The barcoded pyrosequencing analysis of microbial communities across all the 29 samples generated 64 150 quality sequences, with the sequences for individual samples ranging from 634 to 3883 (Table S3). In total, 1226 OTUs were identified in the complete data set, with an average of 53 OTUs per sample. These OTUs had a Chao1 index value ranging from 10 to 331. Over 99% of the OTUs could be assigned to a taxonomic group (phylum) by the RDP classifier (80% threshold). It was evident that the bacterial phylotype richness and phylogenetic diversity in all the pyrites samples were significantly related with pH ($p < 0.01$; Figure S4). In total, 19 phyla were identified. The dominant phyla were *Firmicutes*, *Euryarchaeota*, *Proteobacteria*, and *Nitrospira* (relative abundance >5%), whose sequences accounted for >94% of the total (Figure 1). Additionally, the phyla that were less abundant but still observed in most of the samples included *Actinobacteria* and *Acidobacteria* (Figure 1).

The relative abundance of different phyla varied considerably across the three stages of pyrite oxidation (Figures 1 and S5A). Specifically, the relative abundance of *Firmicutes*, *Proteobacteria*, *Actinobacteria*, and *Bacteroidetes* significantly decreased as the oxidation progressed (Figure S5A). In particular, the relative abundance of *Firmicutes* and *Proteobacteria* decreased from 53% to 27%, and 32% to 3.2%, respectively. By contrast, the relative abundance of *Euryarchaeota* increased dramatically from 0.88% at the early stage to 47% at the final stage (Figure S5A), indicating the important roles of the archaea in pyrite oxidation. These results were consistent with our previous findings that the relative abundance of the archaea increased markedly as the oxidation of pyrite-containing mine tailings progressed.[16,17,39] However, contrasting results have been reported by other researchers. A detailed quantitative real-time PCR and fluorescence in situ hybridization analysis of microbial communities involved in pyrite oxidation found that archaea occurred only in low numbers in the oxidized zones (pH: 3−4) of two pyrite-containing tailings located in Europe.[25] Furthermore, no archaea were detected in the oxidized zone of a pyrite-containing mine tailings in Chile.[49] One possible explanation for this discrepancy was that the low abundance (even disappearance) of the archaea in the mine tailings was likely attributed to the fact that the archaea reported to be relevant for pyrite oxidation are extremophiles,[25] and the pH conditions of the mine tailings were not optimal for the growth of the archaea.

At the genus level, the microbial composition also differed greatly across the three stages of the oxidation and displayed a distinct succession (Figures 2 and S5B). At the early stage, the most dominant genus was *Tumebacillus*, followed by *Thiobacillus*, *Brevundimonas*, *Dyella*, *Alicyclobacillus*, *Rubrobacter*, *Thiomonas*, *Bacillus*, *Sphingomonas*, and *Ferroplasma* (Figure 2). At the mid stage, *Alicyclobacillus* (the fifth most abundant genus at the early stage) became the most dominant genus, whereas the abundance of *Tumebacillus* decreased significantly ($p < 0.05$, Figure S5B) as compared to that at early stage but was still ranked as the second most abundant genus. At the final stage, *Ferroplasma* (whose relative abundances at the two earlier

dx.doi.org/10.1021/es500154z | Environ. Sci. Technol. 2014, 48, 5537−5545

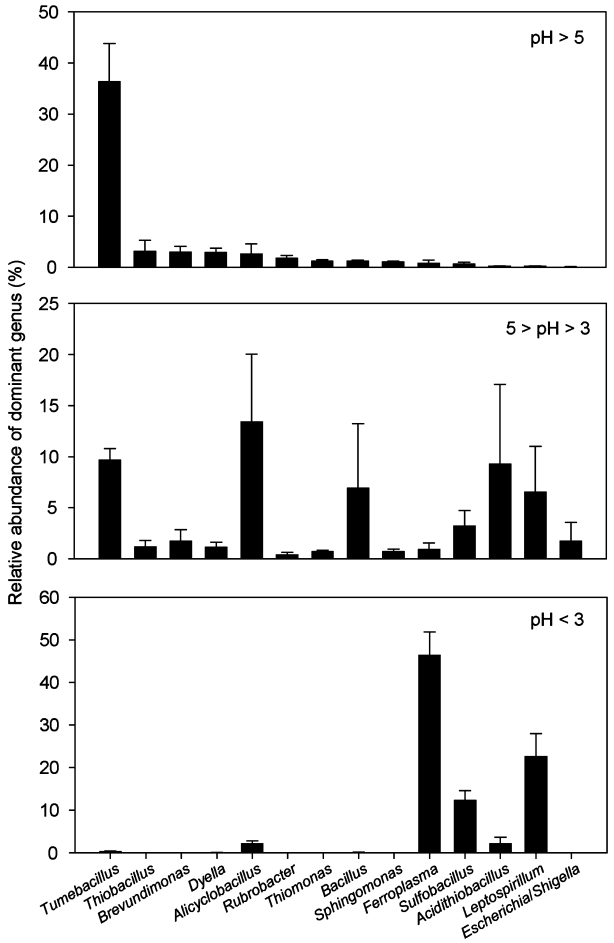

Figure 2. Relative abundance (%) of dominant microbial genera in samples representing the three stages of pyrite oxidation. Those genera with an average abundance of >1% in at least one stage are defined as dominant ones.

stages were about 1%) became the most dominant genus (with a relative abundance of 46%), followed by *Leptospirillum*, *Sulfobacillus*, *Alicyclobacillus*, and *Acidithiobacillus* (Figure 2). Surprisingly, *Tumebacillus* is a newly proposed genus, and only three species of this genus are currently recognized.[61−63] At the present time, there has been no report of the occurrence of this genus in mine environments.[6] However, the numerical dominance of this genus at the first and mid stages highlighted a possibility that *Tumebacillus* is likely to play an important role in sulfur oxidation at the two stages. In support of this, two species of *Tumebacillus* were shown to be able to use sodium thiosulfate and sulfite as sole electron donors,[61,63] leaving another species being untested for its ability in sulfur metabolism.[62] Four additional abundant genera (*Thiobacillus*, *Alicyclobacillus*, *Thiomonas*, and *Ferroplasma*; Figure 2) at the early stage have been reported to include members with sulfur-oxidizing capacity.[6] The predominance of sulfur-oxidizing genera at the early stage indicated that sulfur oxidation was a major biogeochemical process at this stage. In contrast, the genera predominating the final stage were those with members having Fe- or sulfur-oxidizing capacities (*Ferroplasma*, *Leptospirillum*, *Sulfobacillus*, and *Acidithiobacillus*; Figure 2), indicating a possibility that iron and sulfur oxidation occurred at similar intensity at this stage. However, it is worth pointing out that the exceptionally high relative abundance of *Ferroplasma* at the final stage suggests that members of this genus are likely to play a critical role in oxidation of the natural pyrite,[16,17] because they can oxidize Fe^{2+} rapidly into Fe^{3+}, which can attack pyrite directly and widely considered as the most important oxidant for pyrite oxidation.[8] In addition, it could not be excluded that the predominance of *Ferroplasma* was partly attributed to its extremely high tolerance of a low pH, given that the relationship between low pH and % pyrite content is not necessarily directly a proportional one.

Correlations between Geochemical and Microbial Characteristics of Samples Representing the Three Stages of Pyrite Oxidation. The CCA result showed that the abundances of a majority of the dominant microbial genera (including *Ferroplasma*, *Sphingomonas*, *Leptospirillum*, and *Sulfobacillus*) were most closely correlated with EC and pH (see Figure S6 and the Supplementary Note for more details), the changes of which are generally a result of pyrite oxidation. This finding can be largely explained by either the varying pH tolerance of these genera or their involvement in different stages of pyrite oxidation. For example, as mentioned above, the extremely high tolerance of *Ferroplasma* to low pH was likely a cause of the increased predominance of this genus with decreasing pH (Figure S6).

Biogeochemical Model of Sulfide Mineral Oxidation. Combining our results with those from the previous studies,[6,8,9,17] we propose a biogeochemical model of sulfide mineral oxidation (Figure 3 and Table S4), which can facilitate the understanding of the couplings between geochemical, mineralogical, and microbial dynamics. The biogeochemical process is initiated at neutral pH by the release of ferrous iron (Fe^{2+}), which can be easily oxidized into Fe^{3+} by O_2. The ferric iron is then able to oxidize pyrite and other sulfide minerals by reacting with the mineral surface directly. It is widely accepted that Fe-oxidizing microbes can greatly increase the rate of oxidation by regenerating Fe^{3+} efficiently,[8] although there is no consensus as to whether the cells of these microbes are attached to the mineral surface when they are functioning. It should be noted, however, that Fe^{3+} is not soluble in water when the pH is >3.5, where Fe^{3+} will be precipitated as oxyhydroxide. This process releases H^+ and lowers the pH, which will reinitiate the oxidation of sulfide minerals by facilitating Fe^{3+} remaining in solution. On the other hand, some microbes, including *Acidiphilium cryptum*, *Ferribacterium* sp., and *Bacillus* sp., can reduce Fe^{3+} to Fe^{2+}.[6,64] However, the abundance of these microbes tends to decrease as sulfide mineral oxidation progresses (e.g., *Bacillus* sp. in this study, Figure 2). It has been proposed that acid-insoluble (e.g., FeS_2) and acid-soluble (e.g., FeS) sulfide minerals are oxidized through a "thiosulfate mechanism" and a "polysulfide mechanism", respectively.[9] In the thiosulfate mechanism, the most important intermediate product is $S_2O_3^{2-}$, which can be used as an energy source and produce SO_4^{2-} by sulfur-oxidizing microbes, such as *Acidithiobacillus thiooxidans*, *A. caldus*, and *A. ferrooxidans*. In the polysulfide mechanism, the most important intermediate product is S_n^{2-}, which can be either oxidized chemically by Fe^{3+} or biologically by sulfur-oxidizing microbes to rings of elemental sulfur (mainly S_8). S_8 can only be oxidized by sulfur-oxidizing microbes (e.g., *A. ferrooxidans*, *A. thiooxidans*, *A. thiooxidans*, and *A. caldus*) generating SO_4^{2-}. Common to both these two mechanisms is the regeneration of Fe^{2+}, which is oxidized again by Fe-oxidizing microbes, such as *Ferroplasma acidiphilum*, *Leptospirillum ferriphilum*, *L. ferrooxidans*, and *L. ferrodiazotrophum*. As sulfide mineral oxidation progresses, pH

dx.doi.org/10.1021/es500154z | Environ. Sci. Technol. 2014, 48, 5537−5545

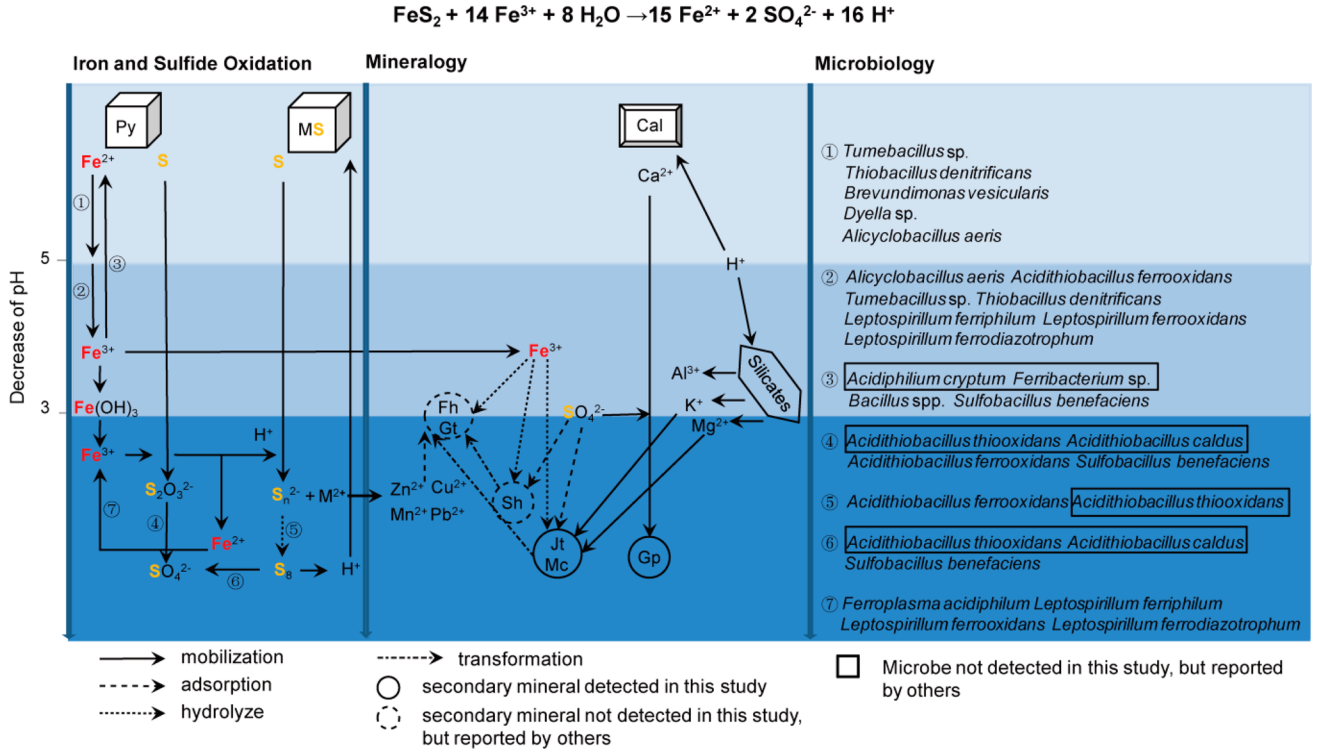

Figure 3. Proposed biogeochemical model of sulfide mineral oxidation. The most relevant microbes found in this study and reported by others are shown. Mineral abbreviations: Cal, calcite; Fh, ferrihydrite; Gp, gypsum; Gt, goethite; Jt, jarosite; Mc, magnesiocopiapite; MS, metal sulfide minerals; Py, pyrite; Sh, schwertmannite.

will greatly decrease, and then divalent cations, SO_4^{2-}, and protons are released. At low pH (<3) under oxidizing conditions, Fe^{3+} can be readily hydrolyzed to form secondary minerals, such as ferrihydrite, goethite, schwertmannite, jarosite, magnesiocopiapite, and other Fe(III) hydroxides.[65] The acid conditions also favor silicates dissolution, which may release the necessary K^+ and Mg^{2+} for jarosite and magnesiocopiapite formation.[66] Zn^{2+}, Cu^{2+}, Mn^{2+}, and Pb^{2+}, generated from oxidation of metal sulfide minerals (e.g., sphalerite, chalcopyrite, and galena), can also form secondary minerals by adsorption. Carbonate minerals (such as calcite) associated with metal sulfide minerals can be dissolved by H^+, so that the relative content of calcite may decrease as the oxidation proceeds, while the released Ca^{2+} can combine with SO_4^{2-} to form gypsum ($CaSO_4$).

In summary, the information gathered here not only improves our understanding of the complex biogeochemical processes governing the natural pyrite oxidation but also has important implications for remediation of acid metalliferous drainage and industrial bioleaching of sulfide minerals. Notwithstanding, there is a clear need to conduct more experiments to confirm our novel finding that the newly proposed genus *Tumebacillus* is likely to play an important role in natural pyrite oxidation. In addition, further study is needed to evaluate the general applicability of the findings of this study, given that the spatial distribution of our samples is more heterogeneous than previously thought. Nevertheless, if the results we observed are indeed general, considering not only the well-known "bioleaching" microbes but also *Tumebacillus*, they offer great promise in both the management of environmental pollution associated with pyrite oxidation and the bioleaching of sulfide minerals.

■ ASSOCIATED CONTENT

Supporting Information

A supplementary note, six figures, and four tables showing additional study details. This material is available free of charge via the Internet at http://pubs.acs.org.

■ AUTHOR INFORMATION

Corresponding Author

*E-mail: shuws@mail.sysu.edu.cn. Fax: +86 20 39332944. Tel.: +86 20 39332933.

Author Contributions

§Y.-t.C and J.-t.L. contributed equally to this work

Notes

The authors declare no competing financial interest.

■ ACKNOWLEDGMENTS

We thank Prof. Alan Baker of The University of Melbourne, the three anonymous reviewers and the editor for their comments that are very useful to improve the quality of this manuscript. We also thank Dr. Jing-ming Wei and Dr. Qi Tao of Guangzhou Institute of Geochemistry for their help in XRD analysis. This work was financially supported by the National Science Foundation of China (nos. 4093212, 31100372 and U1201233) and the Guangdong Provincial Natural Foundation (no. 10451027501005629).

■ REFERENCES

(1) Lundgren, D. G.; Silver, M. Ore leaching by bacteria. *Annu. Rev. Microbiol.* **1980**, *34* (1), 263−283.

(2) Edwards, K. J.; Gihring, T. M.; Banfield, J. F. Seasonal variations in microbial populations and environmental conditions in an extreme

acid mine drainage environment. *Appl. Environ. Microbiol.* **1999**, *65* (8), 3627−3632.
(3) Baker, B. J.; Banfield, J. F. Microbial communities in acid mine drainage. *FEMS Microbiol. Ecol.* **2003**, *44* (2), 139−152.
(4) Johnson, D. B.; Hallberg, K. B. The microbiology of acidic mine waters. *Res. Microbiol.* **2003**, *154* (7), 466−473.
(5) Hallberg, K. B.; González-Toril, E.; Johnson, D. B. *Acidithiobacillus ferrivorans*, sp. nov.; facultatively anaerobic, psychrotolerant iron-, and sulfur-oxidizing acidophiles isolated from metal mine-impacted environments. *Extremophiles* **2010**, *14* (1), 9−19.
(6) Schippers, A.; Breuker, A.; Blazejak, A.; Bosecker, K.; Kock, D.; Wright, T. L. The biogeochemistry and microbiology of sulfidic mine waste and bioleaching dumps and heaps, and novel Fe(II)-oxidizing bacteria. *Hydrometallurgy* **2010**, *104* (3), 342−350.
(7) Edwards, K. J.; Bond, P. L.; Druschel, G. K.; McGuire, M. M.; Hamers, R. J.; Banfield, J. F. Geochemical and biological aspects of sulfide mineral dissolution: lessons from Iron Mountain. *Chem. Geol.* **2000**, *169* (3−4), 383−397.
(8) Schippers, A. Biogeochemistry of metal sulfide oxidation in mining environments, sediments and soils. In *Sulfur biogeochemistry—past and present*; Special Paper 379; Amend, J. P., Edwards, K. J., Lyons, T. W., Eds.; Geological Society of America: Boulder, Colorado, U.S.A., 2004; pp 49−62.
(9) Schippers, A.; Sand, W. Bacterial leaching of metal sulfides proceeds by two indirect mechanisms via thiosulfate or via polysulfides and sulfur. *Appl. Environ. Microbiol.* **1999**, *65* (1), 319−321.
(10) Edwards, K. J.; Goebel, B. M.; Rodgers, T. M.; Schrenk, M. O.; Gihring, T. M.; Cardona, M. M.; Mcguire, M. M.; Hamers, R. J.; Pace, N. R.; Banfield, J. F. Geomicrobiology of pyrite (FeS_2) dissolution: case study at Iron Mountain, California. *Geomicrobiol. J.* **1999**, *16* (2), 155−179.
(11) Larsson, L.; Olsson, G.; Holst, O.; Karlsson, H. T. Pyrite oxidation by *Thermophilic archaebacteria*. *Appl. Environ. Microbiol.* **1990**, *56* (3), 697−701.
(12) Mustin, C.; Berthelin, J.; Marion, P.; De Donato, P. Corrosion and electrochemical oxidation of a pyrite by *Thiobacillus ferrooxidans*. *Appl. Environ. Microbiol.* **1992**, *58* (4), 1175−1182.
(13) Bacelar-Nicolau, P.; Johnson, D. B. Leaching of pyrite by acidophilic heterotrophic iron-oxidizing bacteria in pure and mixed cultures. *Appl. Environ. Microbiol.* **1999**, *65* (2), 585−590.
(14) McGuire, M. M.; Edwards, K. J.; Banfield, J. F.; Hamers, R. J. Kinetics, surface chemistry, and structural evolution of microbially mediated sulfide mineral dissolution. *Geochim. Cosmochim. Acta* **2001**, *65* (8), 1243−1258.
(15) DeSantis, T. Z.; Brodie, E. L.; Moberg, J. P.; Zubieta, I. X.; Piceno, Y. M.; Andersen, G. L. High-density universal 16S rRNA microarray analysis reveals broader diversity than typical clone library when sampling the environment. *Microb. Ecol.* **2007**, *53* (3), 371−383.
(16) Huang, L. N.; Zhou, W. H.; Hallberg, K. B.; Wan, C. Y.; Li, J.; Shu, W. S. Spatial and temporal analysis of the microbial community in the tailings of a Pb-Zn mine generating acidic drainage. *Appl. Environ. Microbiol.* **2011**, *77* (15), 5540−5544.
(17) Chen, L. X.; Li, J. T.; Chen, Y. T.; Huang, L. N.; Hua, Z. S.; Hu, M.; Shu, W. S. Shifts in microbial community composition and function in the acidification process of a lead/zinc mine tailings. *Environ. Microbiol.* **2013**, *15* (9), 2431−2444.
(18) Edwards, R.; Rodriguez-Brito, B.; Wegley, L.; Haynes, M.; Breitbart, M.; Peterson, D.; Saar, M. O.; Alexander, S.; Alexander, E. C., Jr; Rohwer, F. Using pyrosequencing to shed light on deep mine microbial ecology. *BMC Genomics* **2006**, *7*, 57.
(19) Liu, Z. Z.; Lozupone, C.; Hamady, M.; Bushman, F. D.; Knight, R. Short pyrosequencing reads suffice for accurate microbial community analysis. *Nucleic Acids Res.* **2007**, *35* (18), e120.
(20) Yang, C.; Chen, Y.; Peng, P.; Li, C.; Chang, X.; Wu, Y. Trace element transformations and partitioning during the roasting of pyrite ores in the sulfuric acid industry. *J. Hazard. Mater.* **2009**, *167* (1−3), 835−845.
(21) Konhauser, K. O. *Introduction to geomicrobiology*; Blackwell: Oxford, 2007.
(22) Leathen, W. W., Sr.; Braley, S. A.; McIntyre, L. D. The role of bacteria in the formation of acid from certain sulfuritic constituents associated with bituminous coal. II. Ferrous iron oxidizing bacteria. *Appl. Microbiol.* **1953**, *1* (2), 65−68.
(23) Larsson, L.; Olsson, G.; Holst, O.; Karlsson, H. T. Pyrite oxidation by *Thermophilic archaebacteria*. *Appl. Environ. Microbiol.* **1990**, *56* (3), 697−701.
(24) Romero, F. M.; Armienta, M. A.; González-Hernández, G. Solid-phase control on the mobility of potentially toxic elements in an abandoned lead/zinc mine tailings impoundment, Taxco, Mexico. *Appl. Geochem.* **2007**, *22* (1), 109−127.
(25) Kock, D.; Schippers, A. Quantitative microbial community analysis of three different sulfidic mine tailing dumps generating acid mine drainage. *Appl. Environ. Microbiol.* **2008**, *74* (16), 5211−5219.
(26) Fukami, T.; Wardle, D. A. Long-term ecological dynamics: reciprocal insights from natural and anthropogenic gradients. *Proc. R. Soc. London B* **2005**, *272*, 2105−2115.
(27) Tierney, J. E.; Russell, J. M.; Eggermont, H.; Hopmans, E. C.; Verschuren, D.; Sinninghe Damsté, J. S. Environmental controls on branched tetraether lipid distributions in tropical East African lake sediments. *Geochim. Cosmochim. Acta* **2010**, *74* (17), 4902−4918.
(28) Blois, J. L.; Williams, J. W.; Fitzpatrick, M. C.; Jackson, S. T.; Ferrier, S. Space can substitute for time in predicting climate-change effects on biodiversity. *Proc. Natl. Acad. Sci. U.S.A.* **2013**, *110* (23), 9374−9379.
(29) Moses, C. O.; Nordstrom, D. K.; Herman, J. S.; Mills, A. Aqueous pyrite oxidation by dissolved oxygen and by ferric iron. *Geochim. Cosmochim. Acta* **1987**, *51* (6), 1561−1571.
(30) Eggelston, C. M.; Ehrhardt, J.-J.; Stumm, W. Surface structural controls on pyrite oxidation kinetics: an XPS-UPS, STM, and modeling study. *Am. Mineral.* **1996**, *81*, 1036−1056.
(31) Elberling, B.; Schippers, A.; Sand, W. Bacterial and chemical oxidation of pyritic mine tailings at low temperatures. *J. Contam. Hydrol.* **2000**, *41* (3−4), 225−238.
(32) Edwards, K. J.; Hu, B.; Hamers, R. J.; Banfield, J. F. A new look at microbial leaching patterns on sulfide minerals. *FEMS Microbiol. Ecol.* **2001**, *34* (3), 197−206.
(33) Nunan, N.; Wu, K.; Young, I. M.; Crawford, J. W.; Ritz, K. Spatial distribution of bacterial communities and their relationships with the micro-architecture of soil. *FEMS Microbiol. Ecol.* **2003**, *44* (2), 203−215.
(34) Gadd, G. M. Metals, minerals and microbes: geomicrobiology and bioremediation. *Microbiology* **2010**, *156* (3), 609−643.
(35) Zhou, J.; Deng, Y.; Zhang, P.; Xue, K.; Liang, Y.; Van Nostrand, J. D.; Yang, Y.; He, Z.; Wu, L.; Stahl, D. A.; Hazen, T. C.; Tiedje, J. M.; Arkin, A. P. Stochasticity, succession, and environmental perturbations in a fluidic ecosystem. *Proc. Natl. Acad. Sci. U.S.A.* **2014**, DOI: 10.1073/pnas.1324044111.
(36) Tessier, A.; Campbell, P. G. C.; Bisson, M. Sequential extraction procedure for the speciation of particulate trace metals. *Anal. Chem.* **1979**, *51* (7), 844−851.
(37) Chung, F. H. Quantitative interpretation of X-ray diffraction patterns of mixtures. I. Matrix-flushing method for quantitative multicomponent analysis. *J. Appl. Crystallogr.* **1974**, *7* (6), 519−525.
(38) Hubbard, C. R.; Snyder, R. L. Reference intensity ratio—measurement and use in quantitative XRD. *Powder Diffract.* **1988**, *3* (2), 74−78.
(39) Tan, G. L.; Shu, W. S.; Hallber, K. B.; Li, F.; Lan, C. Y.; Zhou, W. H.; Huang, L. N. Culturable and molecular phylogenetic diversity of microorganisms in an open-dumped, extremely acidic Pb/Zn mine tailings. *Extremophiles* **2008**, *12* (5), 657−664.
(40) Bates, S. T.; Berg-Lyons, D.; Caporaso, J. G.; Walters, W. A.; Knight, R.; Fierer, N. Examining the global distribution of dominant archaeal populations in soil. *ISME J.* **2011**, *5* (5), 908−917.
(41) Fierer, N.; Hamady, M.; Lauber, C. L.; Knight, R. The influence of sex, handedness, and washing on the diversity of hand surface bacteria. *Proc. Natl. Acad. Sci. U.S.A.* **2008**, *105* (46), 17994−17999.
(42) Schloss, P. D.; Westcott, S. L.; Ryabin, T.; Hall, J. R.; Hartmann, M.; Hollister, E. B.; Lesniewski, R. A.; Oakley, B. B.; Parks, D. H.;

Robinson, C. J.; Sahl, J. W.; Stres, B.; Thallinger, G. G.; Horn, D. J. V.; Weber, C. F. Introducing mothur: open-source, platform-independent, community-supported software for describing and comparing microbial communities. *Appl. Environ. Microbiol.* **2009**, *75* (23), 7537−7541.
(43) Caporaso, J. G.; Kuczynski, J.; Stombaugh, J.; Bittinger, K.; Bushman, F. D.; Costello, E. K.; Fierer, N.; Peña, A. G.; Goodrich, J. K.; Gordon, J. I.; Huttley, G. A.; Kelley, S. T.; Knights, D.; Koenig, J. E.; Ley, R. E.; Lozupone, C. A.; McDonald, D.; Muegge, B. D.; Pirrung, M.; Reeder, J.; Sevinsky, J. R.; Turnbaugh, P. J.; Walters, W. A.; Widmann, J.; Yatsunenko, T.; Jesse Zaneveld, J.; Knight, R. QIIME allows analysis of high-throughput community sequencing data. *Nat. Methods* **2010**, *7* (5), 335−336.
(44) DeSantis, T. Z.; Hugenholtz, P.; Keller, K.; Brodie, E. L.; Larsen, N.; Piceno, Y. M.; Phan, R.; Andersen, G. L. NAST: a multiple sequence alignment server for comparative analysis of 16S rRNA genes. *Nucleic Acids Res.* **2006**, *34* (suppl 2), W394−W399.
(45) Wang, Q.; Garrity, G. M.; Tiedje, J. M.; Cole, J. R. Naive Bayesian classifier for rapid assignment of rRNA sequences into the new bacterial taxonomy. *Appl. Environ. Microbiol.* **2007**, *73* (16), 5261−5267.
(46) ter Braak, C. J. F. Canonical correspondence analysis: a new eigenvector method for multivariate direct gradient analysis. *Ecology* **1986**, *67* (5), 1167−1179.
(47) Boon, M.; Brasser, H. J.; Hansford, G. S.; Heijnen, J. J. Comparison of the oxidation kinetics of different pyrites in the presence of *Thiobacillus ferrooxidans* or *Leptospirillum ferrooxidans*. *Hydrometallurgy* **1999**, *53* (1), 57−72.
(48) Okibe, N.; Johnson, D. B. Biooxidation of pyrite by defined mixed cultures of moderately thermophilic acidophiles in pH-controlled bioreactors: significance of microbial interactions. *Biotechnol. Bioeng.* **2004**, *87* (5), 574−583.
(49) Diaby, N.; Dold, B.; Pfeifer, H. R.; Holliger, C.; Johnson, D. B.; Hallberg, K. B. Microbial communities in a porphyry copper tailings impoundment and their impact on the geochemical dynamics of the mine waste. *Environ. Microbiol.* **2007**, *9* (2), 298−307.
(50) Mikkelsen, D.; Kappler, U.; Webb, R. I.; Rasch, R.; McEwan, A. G.; Sly, L. I. Visualisation of pyrite leaching by selected thermophilic archaea: nature of microorganism—ore interactions during bioleaching. *Hydrometallurgy* **2007**, *88* (1), 143−153.
(51) Larsen, F.; Postma, D. Nickel mobilization in a groundwater well field: release by pyrite oxidation and desorption from manganese oxides. *Environ. Sci. Technol.* **1997**, *31* (9), 2589−2595.
(52) McGregor, R. G.; Blowes, D. W. The physical, chemical and mineralogical properties of three cemented layers within sulfide-bearing mine tailings. *J. Geochem. Explor.* **2002**, *76* (3), 195−207.
(53) Pagnanelli, F.; Moscardini, E.; Giuliano, V.; Toro, L. Sequential extraction of heavy metals in river sediments of an abandoned pyrite mining area: pollution detection and affinity series. *Environ. Pollut.* **2004**, *132* (2), 189−201.
(54) Fernández-Remolar, D. C.; Morris, R. V.; Gruener, J. E.; Amils, R.; Knoll, A. H. The Río Tinto Basin, Spain: mineralogy, sedimentary geobiology, and implications for interpretation of outcrop rocks at Meridiani Planum, Mars. *Earth. Planet. Sci. Lett.* **2005**, *240* (1), 149−167.
(55) Appelo, C. A. J.; Verweij, E.; Schafer, H. A hydrogeochemical transport model for an oxidation experiment with pyrite/calcite/exchangers/organic matter containing sand. *Appl. Geochem.* **1998**, *13* (2), 257−268.
(56) Agnew, M.; Taylor, G. *The development, cycling and effectiveness of hardpans and cemented layers in tailings storage facilities in Australia*; The 4th AMD Workshop: Townsville, Australia, February 28−March 2, 2000.
(57) Coskren, T. D.; Lauf, R. J. The minerals of Alum Cave Bluff, Great Smoky Mountains, Tennessee. *Mineral. Rec.* **2000**, *31* (2), 163−175.
(58) Hammarstrom, J. M.; Seal, R. R., II; Meier, A. L.; Kornfeld, J. M. Secondary sulfate minerals associated with acid drainage in the eastern U.S.: recycling of metals and acidity in surficial environments. *Chem. Geol.* **2005**, *215* (1), 407−431.
(59) McKibben, M. A.; Barnes, H. L. Oxidation of pyrite in low temperature acidic solutions: rate laws and surface textures. *Geochim. Cosmochim. Acta* **1986**, *50* (7), 1509−1520.
(60) Druschel, G. K.; Baker, B. J.; Gihring, T. M.; Banfield, J. F. Acid mine drainage biogeochemistry at Iron Mountain, California. *Geochem. Trans.* **2004**, *5* (2), 13−32.
(61) Steven, B.; Chen, M. Q.; Greer, C. W.; Whyte, L. G.; Niederberger, T. D. *Tumebacillus permanentifrigoris* gen. nov., sp. nov., an aerobic, spore-forming bacterium isolated from Canadian high Arctic permafrost. *Int. J. Syst. Evol. Microbiol.* **2008**, *58* (6), 1497−1501.
(62) Baek, S. H.; Cui, Y.; Kim, S. C.; Cui, C. H.; Yin, C.; Lee, S. T.; Im, W. T. *Tumebacillus ginsengisoli* sp. nov., isolated from soil of a ginseng field. *Int. J. Syst. Evol. Microbiol.* **2011**, *61* (7), 1715−1719.
(63) Wang, Q.; Xie, N.; Qin, Y.; Shen, N.; Zhu, J.; Mi, H.; Huang, R. *Tumebacillus flagellatus* sp. nov., an α-amylase/pullulanase-producing bacterium isolated from cassava wastewater. *Int. J. Syst. Evol. Microbiol.* **2013**, *63* (9), 3138−3142.
(64) Johnson, D. B.; Kanao, T.; Hedrich, S. Redox transformations of iron at extremely low pH: fundamental and applied aspects. *Front. Microbiol.* **2012**, *16* (3), 96.
(65) Dold, B.; Fontboté, L. Element cycling and secondary mineralogy in porphyry copper tailings as a function of climate, primary mineralogy, and mineral processing. *J. Geochem. Explor.* **2001**, *74* (1), 3−55.
(66) Farquhar, M. L.; Vaughan, D. J.; Hughes, C. R.; Charnock, J. M.; England, K. E. Experimental studies of the interaction of aqueous metal cations with mineral substrates: lead, cadmium, and copper with perthitic feldspar, muscovite, and biotite. *Geochim. Cosmochim. Acta* **1997**, *61* (15), 3051−3064.